Structures 71 (2025) 108074

Contents lists available at ScienceDirect

Structures

journal homepage: www.elsevier.com/locate/structures

Experimental and numerical study of an elliptical roller damper under cyclic loading

Hadis Vakili Sadeghi [a], Nader Fanaie [a,*], Majid Latifi [b]

[a] Department of Civil Engineering, K. N. Toosi University of Technology, Tehran, Iran
[b] Foolad Machine Industry, Neka, Iran

ARTICLE INFO

Keywords:
Yielding damper
Elliptical roller damper
Gravity loads
Cyclic loading
Parametric analysis

ABSTRACT

This paper presents a detailed experimental and numerical investigation of a novel structural control device termed the Elliptical Roller Damper. This innovative damper integrates rollers into the conventional elliptical damper, a yielding type, enabling it to sustain substantial gravity loads. This capability notably alleviates the dead load imposed on other components within the gravity load-bearing system. Initially, two prototypes of the damper were subjected to cyclic displacement-controlled loading, demonstrating stable hysteresis curves characterized by significant energy dissipation capabilities. Further experimental evaluations under varied gravity loads affirmed that these loads exert negligible impact on the operational effectiveness of the damper. Numerical simulations were performed using the finite element software Abaqus to explore additional parameters influencing the damper's behavior. It was ascertained that the friction coefficient does not substantially affect the damper's lateral strength. However, modifications in the material properties, particularly the adoption of higher-strength steel, markedly enhance the lateral strength of the damper. Additionally, alterations in the geometric configuration of the damper were analyzed. The results indicated that increasing the thickness of the elliptical section and reducing its height significantly bolstered the lateral strength of the damper. Quantitatively, the enhancements in strength were exponential to the adjustments in thickness, and disproportionately greater relative to the changes in height. In contrast, modifications to the length of the flat section were found to be inconsequential, while adjustments to the width modestly influenced the damper's performance. The relationship between changes in strength and width alterations was linear.

1. Introduction

In recent decades, structural engineers have increasingly embraced innovative methodologies to augment the seismic resilience of structures. Among these methodologies, the adoption of yielding dampers stands out due to their capacity to absorb and dissipate the kinetic energy released during seismic events. Yielding dampers operate as a crucial component of displacement-dependent passive control systems, engaging the plastic deformation range to dissipate energy effectively [1,2].

The concept of yielding dampers was initially introduced by Kelly et al. in 1972, marking a significant advancement in seismic mitigation technologies [3]. This innovation was subsequently refined through further research in 1974 [4]. Yielding dampers offer several distinct advantages that have captured the interest of the engineering community. These include autonomous operation without the necessity for external energy sources, the production of stable hysteresis cycles, straightforward installation procedures, and the ability to replace the dampers in post-seismic events. Additionally, these devices are characterized by their insensitivity to temperature variations and cost-effectiveness, further enhancing their appeal.

One of the earliest implementations of yielding dampers is the U-shaped damper, which is fabricated by bending a metal sheet into a U configuration. This design strategy is aimed at mitigating stress concentrations, thereby enhancing the damper's efficacy and durability. U-shaped dampers are noted for their simple design, economical production, versatile application possibilities, and ease of replacement. By juxtaposing two U-shaped dampers and securing them together, an elliptical damper configuration is achieved, as depicted in Fig. 1.

When force is exerted on an elliptical damper system, reciprocating movements predominantly occur within the curved segments, while the straight segments retain their original form. These curved segments are

* Correspondence to: K. N. Toosi University of Technology, Department of Civil Engineering, No. 1346, Vali-Asr Street, P.O. Box. 15875-4416, Tehran 19697, Iran.
E-mail address: fanaie@kntu.ac.ir (N. Fanaie).

https://doi.org/10.1016/j.istruc.2024.108074
Received 15 August 2024; Received in revised form 18 November 2024; Accepted 15 December 2024
Available online 8 January 2025

Fig. 1. Combination of Two U-Shaped Dampers and the Construction of an Elliptical Damper.

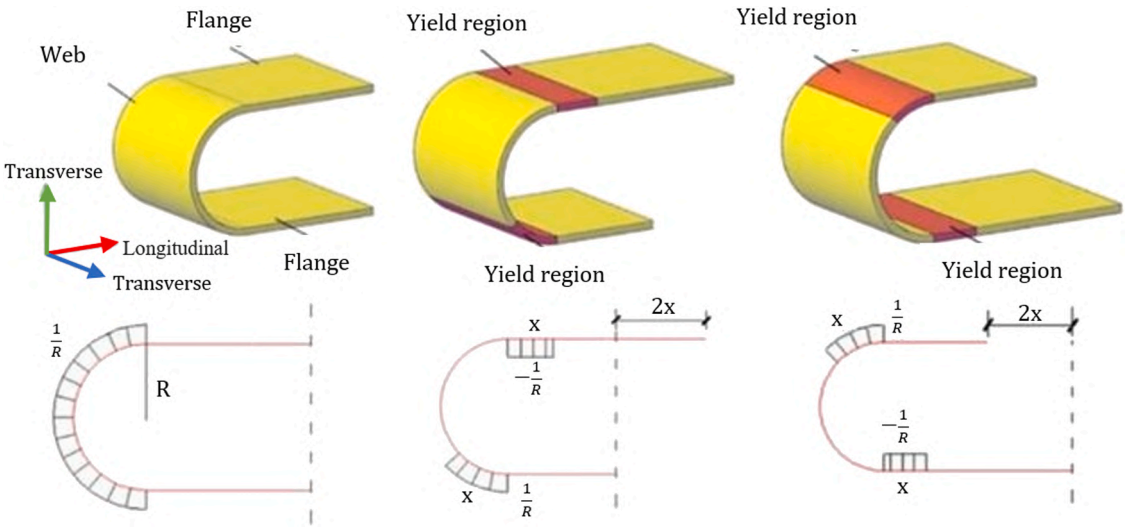

Fig. 2. The Mechanism of U-Shaped Dampers Under Loading [5].

Fig. 3. Details of the Experiment Conducted on One of the Dampers Presented by Kim et al. [8].

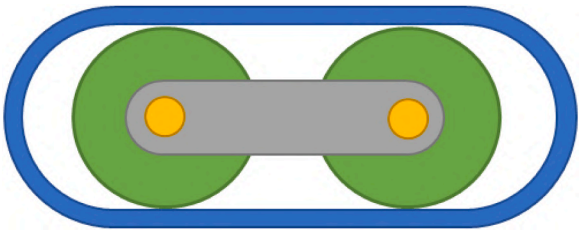

Fig. 4. Elliptical Roller Damper.

intentionally designed as the principal components for energy dissipation, achieving this through plastic deformations. As the damper undergoes deformation, the upper and lower straight profiles undergo alternate extension and compression in opposite directions, contributing to the overall energy dissipation mechanism.The curved sections primarily dissipate the incoming energy through combined flexural and shear deformations. Additionally, due to axial movements at both termini of the damper, the yielding sections along the straight profiles are activated to mitigate plastic concentration. This activation enhances the damper's capacity to dissipate energy. These dynamic movements facilitate the distribution of stress concentrations, ensuring they do not remain localized but rather migrate along the curved section. This migration results in a continuous variation in the yield point. (Fig. 2) [5]

In other words, in contrast to other yielding systems where strains are typically extensive and localized at specific points, the design of these dampers ensures that strains are minimized and their locations continuously shift. This dynamic displacement of the maximum stress point is crucial, as it allows the damper to sustain its functionality across

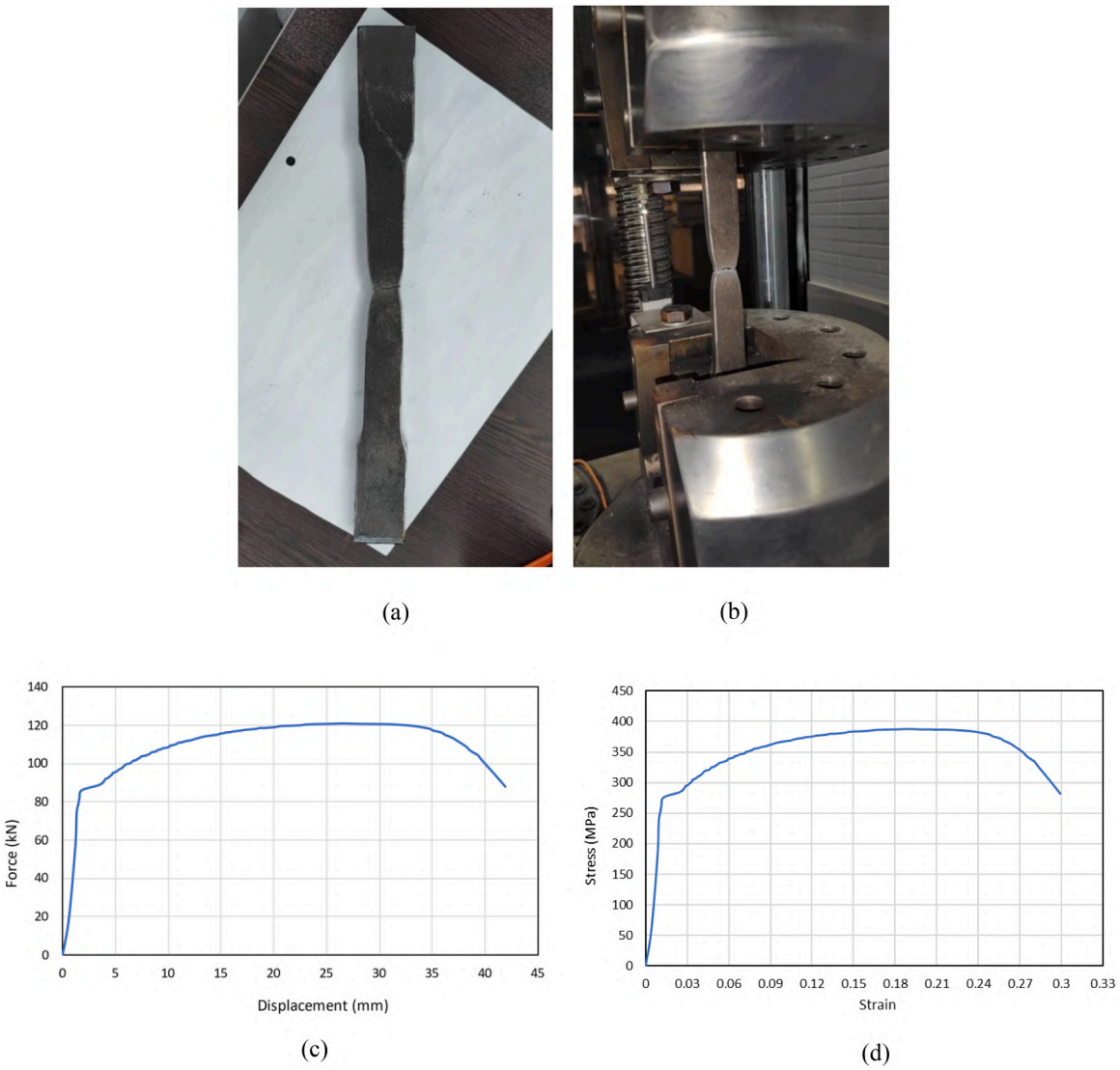

Fig. 5. Tensile Test on Utilized Steel: (a) Test Sample After Copoun Test, (b) End of Copoun Test, (c) Force-Displacement Curve, (d) Stress-Strain Curve.

numerous cycles and postpone the onset of fatigue. This characteristic represents a substantial advantage of this system, addressing and mitigating common weaknesses found in many other dampers, such as localized strain concentrations at a single point and susceptibility to fatigue phenomena.

Recent studies have focused extensively on U-shaped dampers. Baird et al. have created equations that predict how these dampers behave under different force and displacement scenarios [6]. Additionally, Deng et al. introduced a method for calculating the energy dissipation ratio, helping engineers understand how efficient these dampers are during seismic activities [7].

Kim and his team developed three models of high-dissipation dampers. Their third model, which features closed-loop curves and surfaces (Fig. 3), stood out because it showed better ductility and was able to dissipate more energy under cyclic shear loading. Importantly, this model did not lose strength after yielding, which is crucial for maintaining structural integrity during and after earthquakes [8].

In 2019, Taiyari et al. introduced a buckling brace that incorporated U-shaped dampers, showcasing its effectiveness through cyclic tests. These tests confirmed the damper's high energy dissipation capacity and its ability to maintain stable behavior under nonlinear displacements [9]. Following this, Mezzolani and colleagues integrated both this new damper and the conventional U-shaped damper into a steel frame to compare their performance. Their findings highlighted that the innovative damper significantly improved the reduction of both relative and absolute interstory drift, enhancing the frame's structural stiffness compared to the classic damper [10].

Lee et al. conducted experiments on five elliptical dampers of varying dimensions to examine characteristics such as initial stiffness, post-yield stiffness ratio, ultimate strength, ultimate displacement, and ductility. They determined that reducing the length of the straight section and decreasing the radius of curvature could enhance strength and minimize displacement [11]. Similarly, Gao and colleagues explored the mechanical properties of U-shaped dampers by altering the length of the straight section, the radius of the curved section, and the shape of the curved section (convex vs. concave) under tensile and compressive

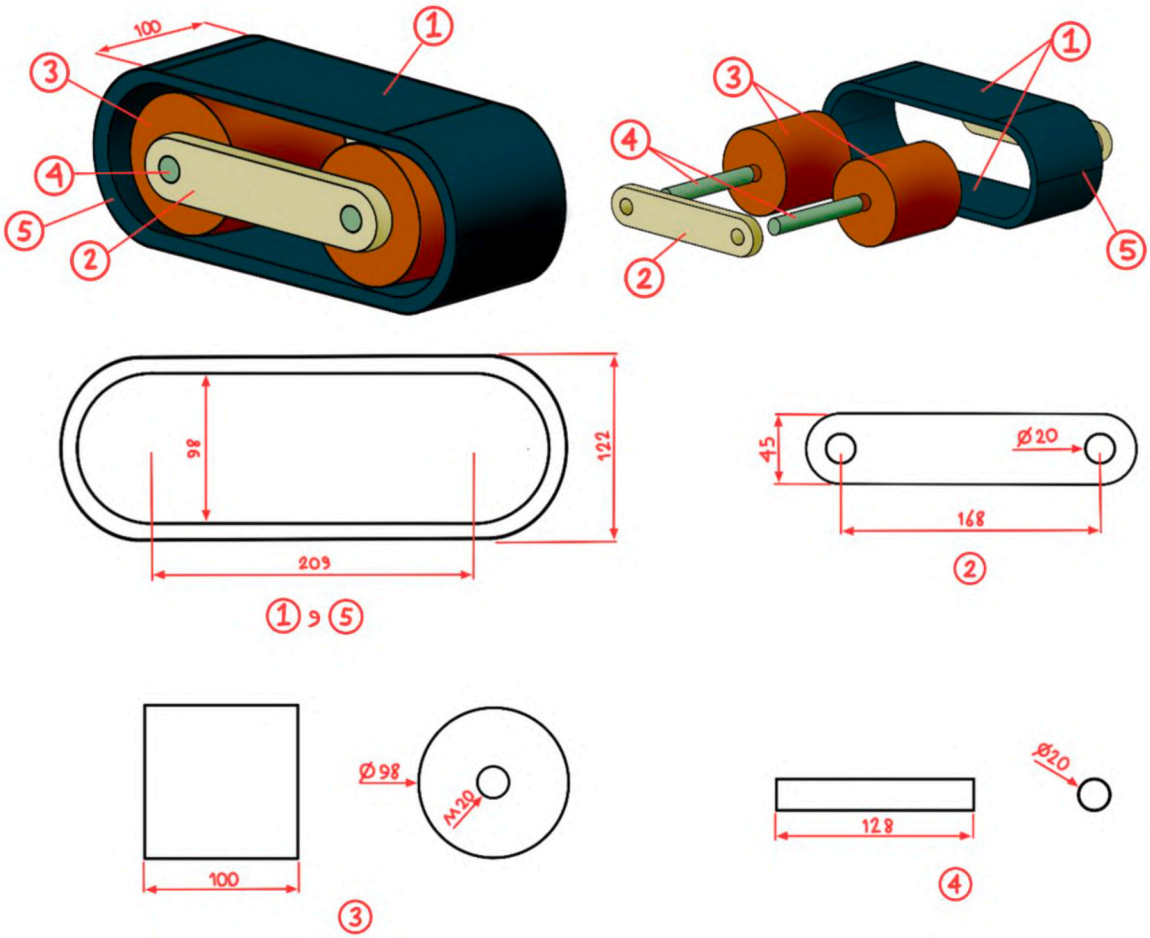

Fig. 6. Geometry of Elliptical Roller Damper.

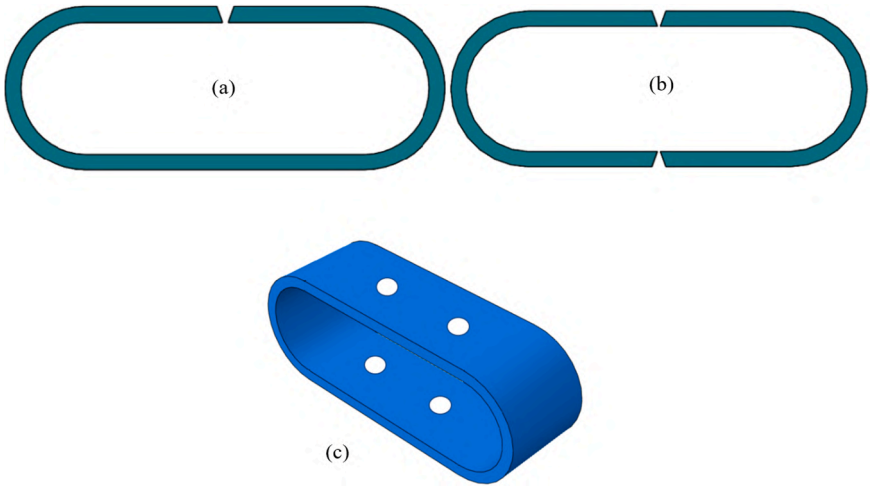

Fig. 7. Welding Locations of the Elliptical Damper: (a) First Method (b) Second Method (c) Locations of the Holes.

forces [12].

Satria et al. in 2021 utilized finite element software to study the elastic stiffness, maximum strength, and energy dissipation of various configurations of U-shaped steel dampers. Their research indicated that symmetrical dampers tend to dissipate more energy. Additionally, arranging more U-shaped components horizontally was found to bolster stiffness and strength, whereas increasing them vertically led to higher elastic deformation but reduced elastic stiffness and strength [13].

U-shaped dampers have many applications in various structural systems, which researchers have studied extensively. The innovative elliptical roller damper can also be implemented in frames, walls, and seismic isolators.

Research on the application of U-shaped and elliptical dampers in frames has been extensively explored by researchers. Ebadi et al. implemented these dampers in 4 and 8-story steel frames, observing reductions in inter-story drift and shear between floors [14].

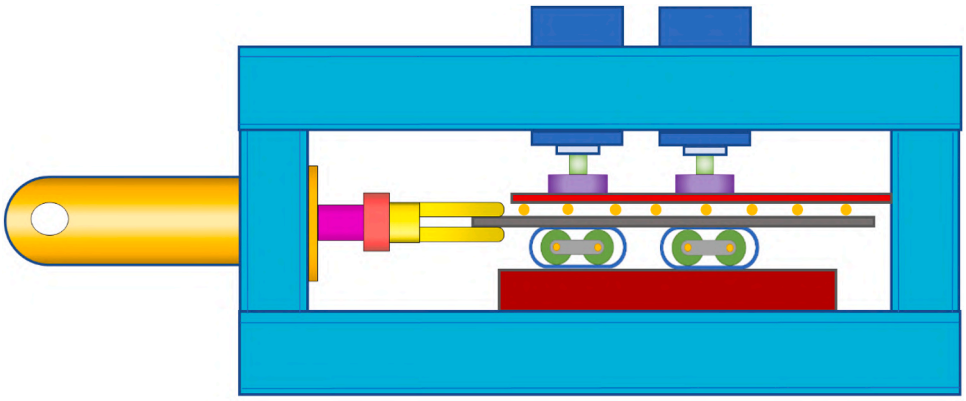

Fig. 8. Test Setup.

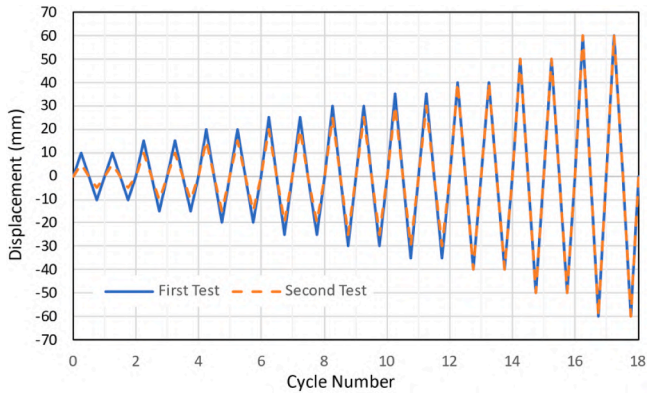

Fig. 9. Loading Protocol.

Bakhshpoori and co-workers analyzed these dampers in 5, 10, and 15-story concrete frames subjected to 7 earthquake records. The results showed that the use of dampers reduced relative floor displacement and maximum roof displacement, thereby enhancing the performance level of the frames [15]. Further analysis by Bagheri and colleagues contrasted U-shaped yielding dampers with rotational friction dampers across steel buildings of three, five, and ten stories. They concluded that while friction dampers more effectively reduced base shear, U-shaped dampers better minimized roof displacement [16]. Chen and team introduced a novel elliptical metal damper designed with dual yield points, which they showed to significantly enhance seismic resistance in a reinforced concrete building under time history analysis [17]. Najari Varzaneh et al. explored the effectiveness of a ring damper in a single-story steel frame using Abaqus software. Their findings demonstrated that these dampers not only preserved the elastic state of the structure but also improved its ductility and energy absorption [18]. Najafi et al. conducted comparative studies on circular, elliptical, and T-ADAS dampers in Chevron bracing, utilizing Abaqus finite element software to identify the optimal damper configuration [19]. Bursi and his team innovated by incorporating four quarter-circle rings into a cable-damper system, which increased initial stiffness, ultimate strength, and reduced pinching effects in hysteresis cycles [20].

Additionally, Maleki et al. embarked on four separate studies examining various types of pipe dampers—single, double, and concrete-filled—and their applications in different structures like bridges [21–24].

The use of U-shaped and elliptical dampers in seismic isolators has been the focus of significant research efforts. Initially, Suzuki et al. evaluated the potential of these dampers in isolators by testing a U-shaped damper under 360-degree force applications at varying speeds and temperatures. Their findings indicated that the stiffness and strength of the dampers remained consistent regardless of the force applied, and the dampers showed stable hysteresis behavior across different conditions [25].

Building on this foundation, Oh and colleagues conducted experiments on a two-story building model equipped with a damper on a shake table. They found that the isolator not only increased the structural period but also effectively concentrated deformations at the ground floor, thus reducing seismic demand [26]. More recently, in 2021, a study involving a seismic isolator paired with a U-shaped damper in a 5-story building under both seismic and blast loads was performed using nonlinear time history analysis. The results from this study highlighted that the combined use of the isolator and damper significantly lowered base shear, top-floor accelerations, and overall structural deformations [27].

Additionally, the integration of U-shaped dampers into concrete shear walls has also been investigated. Henry et al. explored using these dampers to connect concrete shear walls to structural frames, aiming to enhance the seismic strength of the walls [28]. Furthermore, Kim and his team studied the incorporation of U-shaped dampers in link beams of reinforced concrete shear walls [29].

2. Elliptical roller damper

The elliptical roller damper, illustrated in Fig. 4, is highlighted as a novel development in this paper. This innovation enhances the traditional elliptical yielding damper by incorporating multiple rollers. These rollers are designed to support both gravitational and seismic loads, serving dual functions: they not only dissipate dynamic energy generated by earthquakes but also help carry the static weight of the structure. This dual capability of the elliptical roller damper significantly reduces the transmission of seismic energy to the structure and improves overall structural stability.

The rollers integrated within the elliptical damper serve a multifunctional role. They are crucial not just for bearing or transmitting gravitational loads but also for controlling deformations during seismic events. The diameter of each roller is specifically sized to fit the internal dimensions of the damper, and they are designed to be stiffer than the

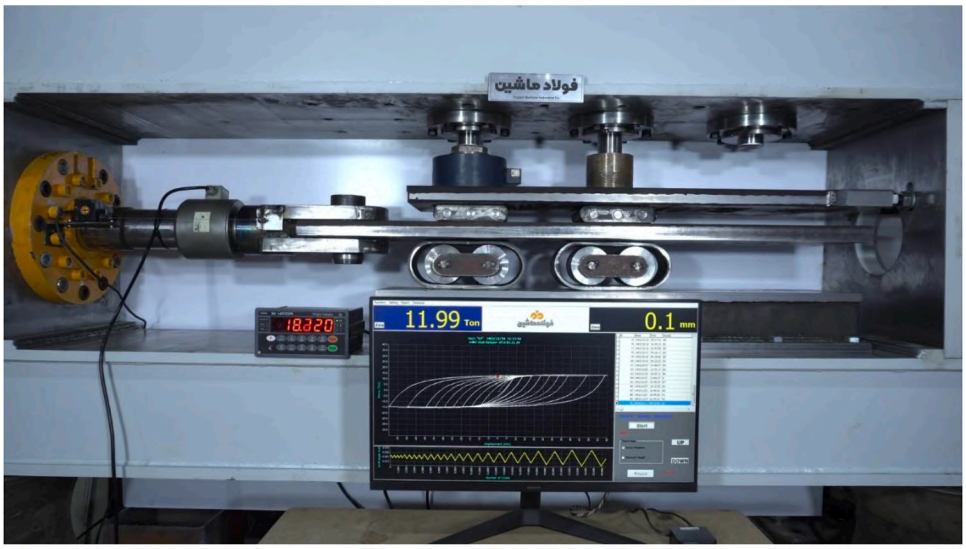

(a)

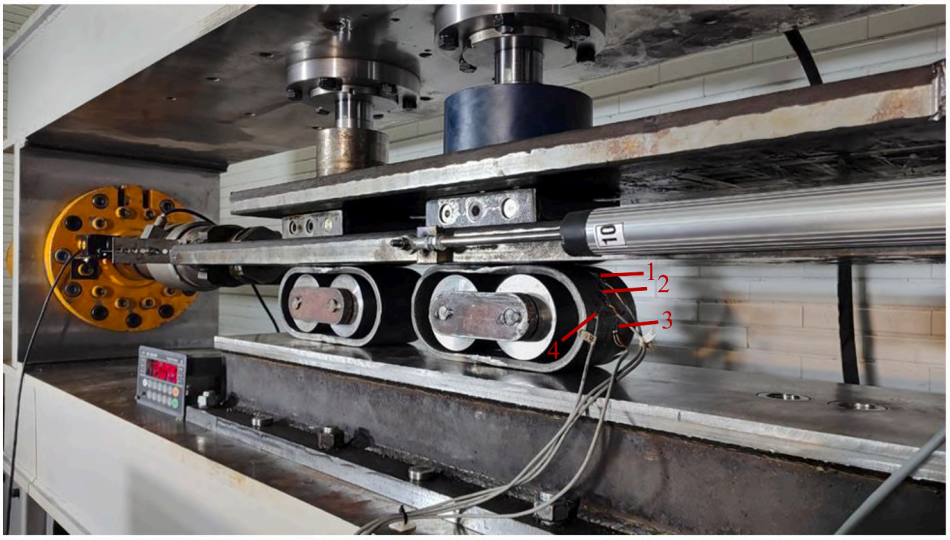

(b)

Fig. 10. End of Experiment: (a) First Test, (b) Second Test.

materials used in the elliptical sections. This configuration ensures that the rollers positively influence the damper's performance during horizontal displacements.

The decision on the number of rollers used in this innovative damper is strategically based on the magnitude of gravitational load the damper is expected to manage. Opting against the use of a single roller is a deliberate design choice; a solitary roller tends to increase the risk of misalignment or deviation from the axis of motion during dynamic shifts. By employing two or more rollers, the damper not only boosts its load-bearing capacity but also achieves a more even distribution of forces across a larger surface area, effectively eliminating the issue of roller misalignment.

3. Experimental study

To initiate the experiment, selecting the appropriate material for the damper is crucial. The metal chosen for these dampers must exhibit suitable hysteresis behavior, endure a wide fatigue range, possess relatively high strength, and maintain low sensitivity to temperature variations. For this experiment, steel ST37 was selected due to its favorable properties. After acquiring the steel, a tensile test was conducted on a dog bone sample with gauge length equal to 140 mm to accurately chart its stress-strain curve, as depicted in Fig. 5. The initial area of the sample was 312 mm^2. Fig. 5(a) and (b) show the ST37 steel specimen at the final stage of the tensile test, where necking and localized deformation are clearly visible. This test was essential for determining precise mechanical properties such as yield stress and strain, ultimate stress, and fracture strain as shown in Fig. 5(c) and (d) [30,31].

The selected dimensions for this damper are detailed in Fig. 6. The damper comprises several key components:

1. Flat Plates
2. Connecting Plates
3. Rollers
4. Pins
5. Curved Sections

Specifically, the elliptical section, combining both flat and curved

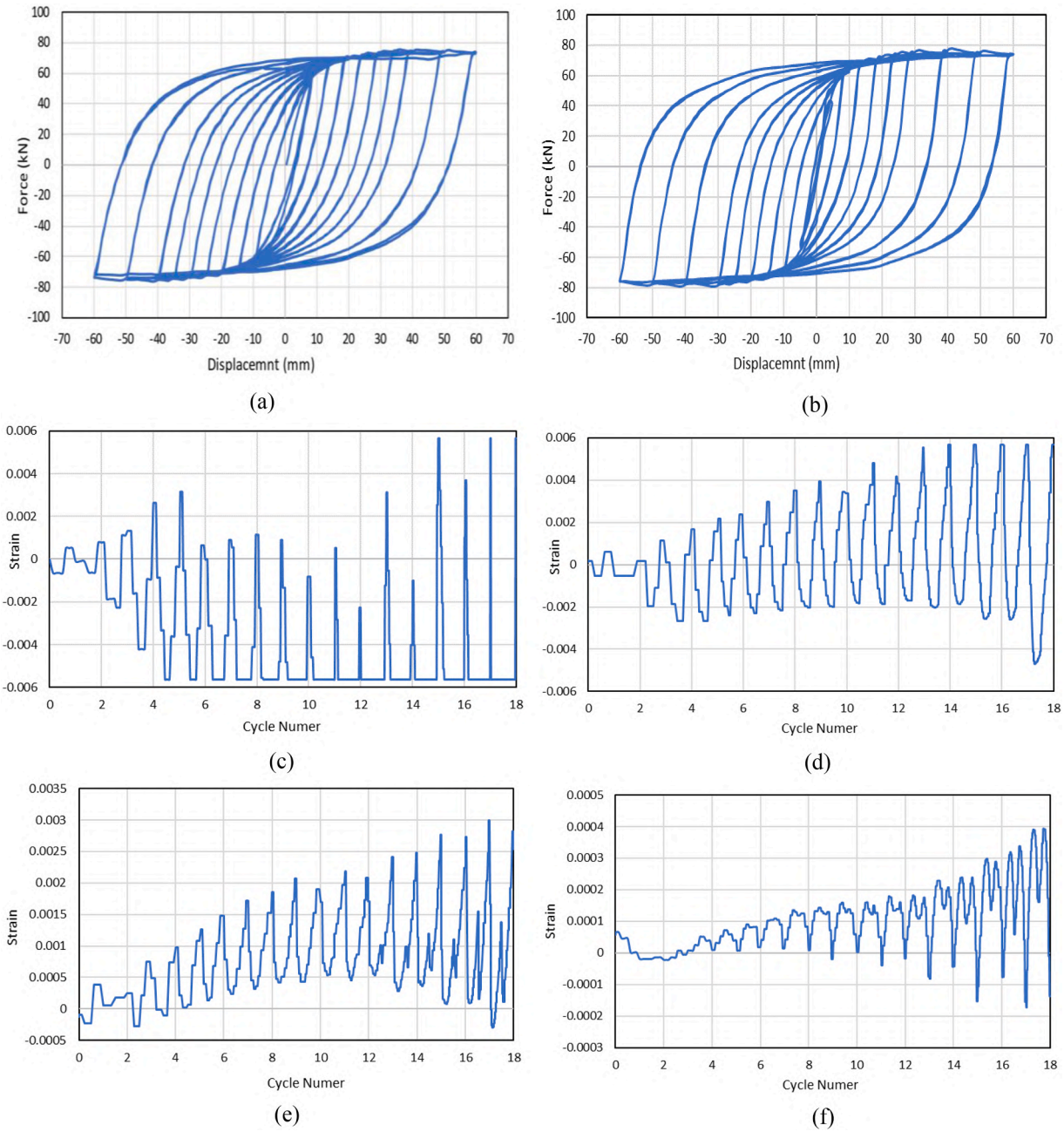

Fig. 11. Experimental Curves: (a) First Test Hysteresis Curve, (b) Second Test Hysteresis Curve, (c) Result of Strain Gauge 1, (d) Result of Strain Gauge 2, (e) Result of Strain Gauge 3, (f) Result of Strain Gauge 4.

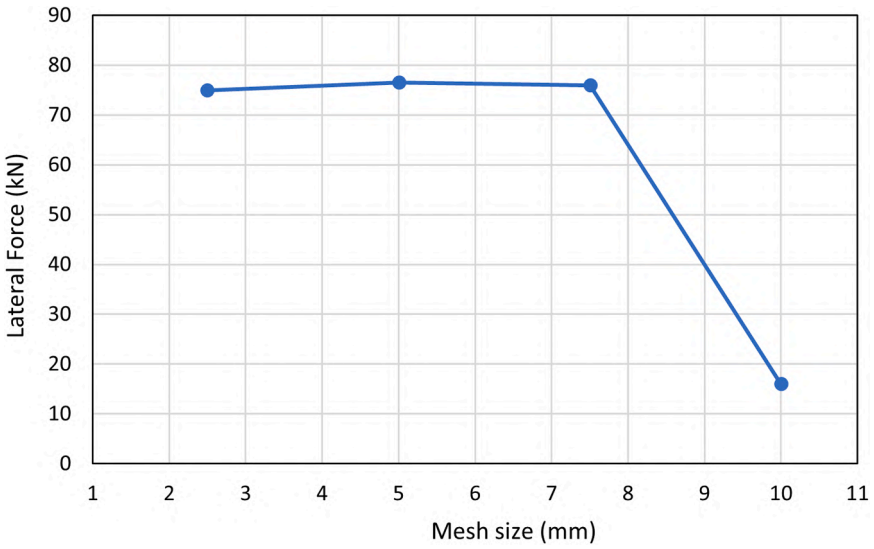

Fig. 12. Mesh Sensivity Analysis.

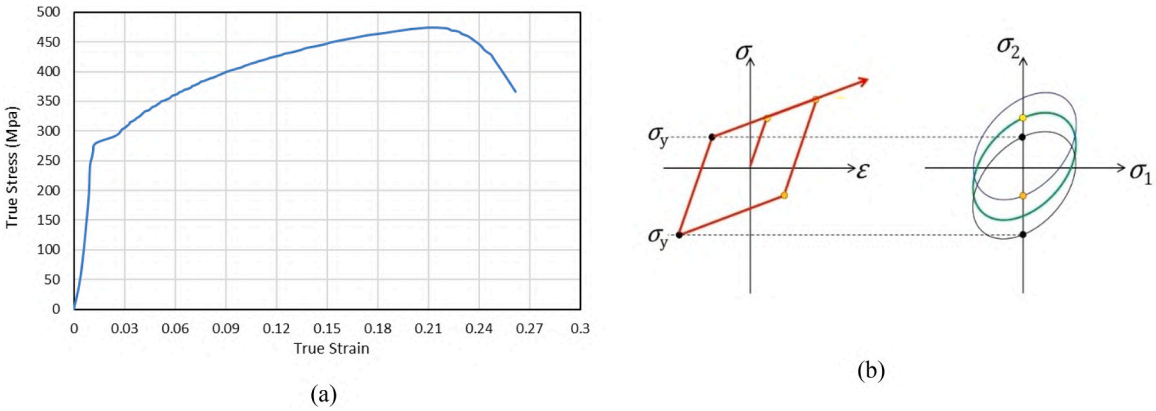

Fig. 13. Material Model in Abaqus: (a) True Stress-Strain Curve, (b) Kinematic Hardening Model.

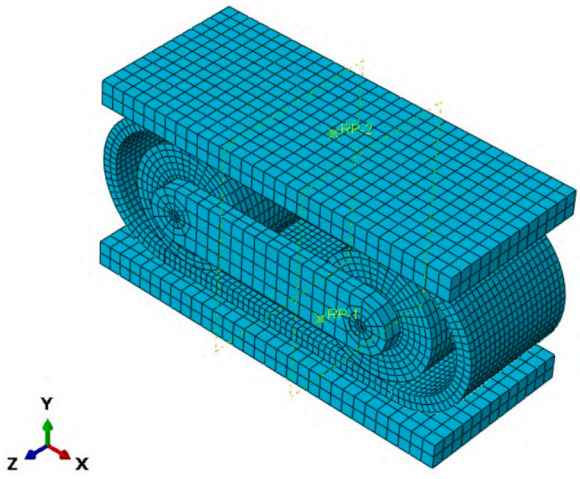

Fig. 14. Numerical Model of Damper.

plates, measures 331 mm in length, 122 mm in height, 100 mm in width, and has a thickness of 12 mm. The rollers are designed with a diameter of 98 mm and match the elliptical section's width at 100 mm. Additionally, the pins used to secure the rollers and other components have a diameter of 20 mm and a length of 128 mm. The connecting plate that holds the rollers together will be 213 mm long, 45 mm high, and 14 mm thick.

To fabricate the elliptical section, which comprises the flat and curved plates, two construction techniques are outlined in Fig. 7. The first method entails bending a single plate—either through cold or hot forming—and securing it with a full penetration groove weld at the center of either the upper or lower flat plate. The second method involves assembling two U-shaped sections facing each other, connected at their bases with a full penetration groove weld, as depicted in Fig. 7. For this experiment, the second method was selected.

In this chosen method, the flat plates are connected to the loading plate using two pins. It is important to ensure that these pins are not located in the curved sections of the damper. The dynamic, reciprocating movements and the potential stress concentration in these areas could result in damper failure through either pin or weld fractures. Therefore, the pin passing holes were embedded in the flat plate as shown in Fig. 7 (c). Additionally, the rollers are interconnected via a plate known as the connecting plate. Each roller is attached to this plate with a press-fitted pin to maintain structural integrity.

In the laboratory at Foolad Machine factory, four dampers constructed from steel ST37, following the dimensions outlined in Fig. 6, were assembled and positioned according to the setup shown in Fig. 8 two by two in two separated test. To simulate the weight of a building, a 180 kN gravitational load was applied to each damper using two vertical

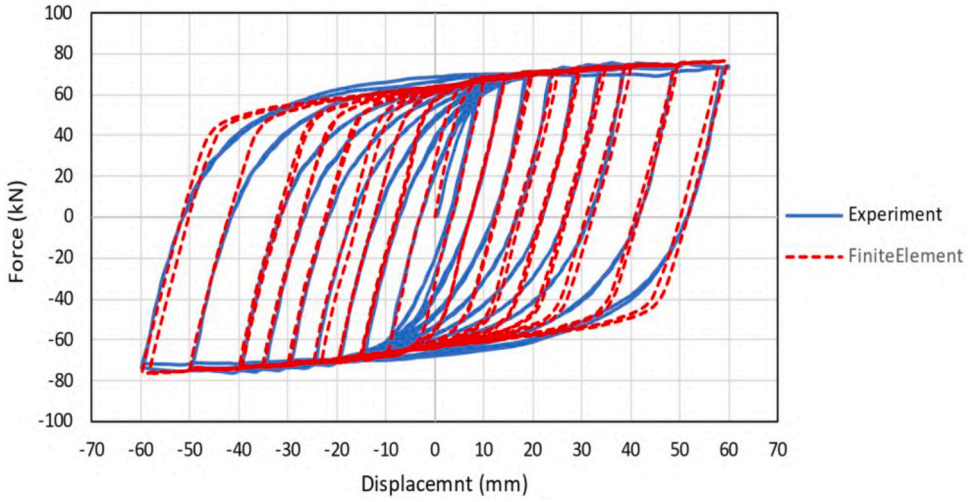

Fig. 15. Comparison of the Hysteresis Curves from Abaqus and the Experiment.

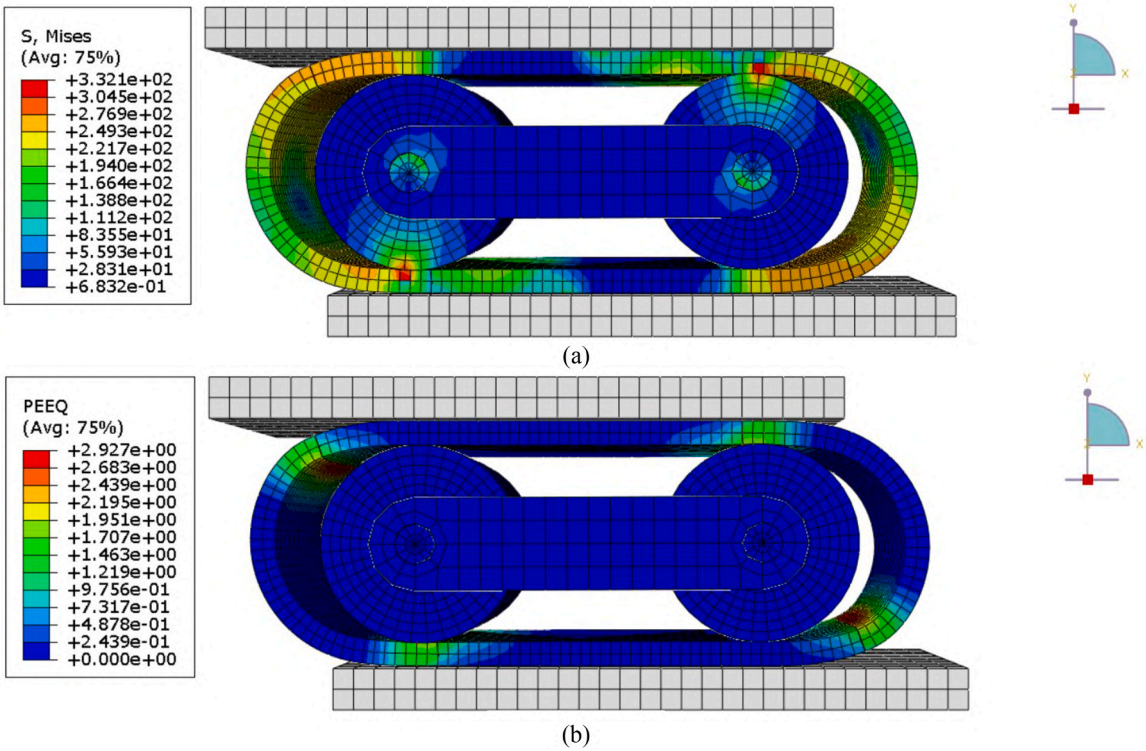

Fig. 16. Contour of the Damper after Analysis at Maximum Displacement (a) Von Mises Stress Contour in MPa, (b) Equivalent Plastic Strain Contour.

actuators capable of exerting a force of 300 kN. However, the load cell is connected to only one of the actuators, and the value displayed on the monitor corresponds to just one of the actuators. The capacity of load cell is 1000 kN with accuracy of 0.1 kN. Additionally, to mimic the lateral forces that a building might experience during seismic activity, lateral loading was applied using a horizontal actuator which has 400 kN capacity.

The lateral loading on the damper is applied using a quasi-static cyclic method and displacement control. As illustrated in Fig. 9, the process begins with the application of two identical cycles, each inducing a displacement of 10 mm, executed using a hydraulic actuator. Following the guidelines set forth in FEMA 461 [32], the displacement is then increased incrementally—by a maximum of 40 % of the previous displacement every two cycles. This incremental increase continues until the damper achieves a maximum displacement of 60 mm. In the second test, we removed two mid-level cycles and introduced two additional cycles at a 5 mm displacement.

Ultimately, the two constructed dampers underwent a test involving horizontal displacement across 18 cycles. During this test, the lateral load-bearing capacity, or lateral strength, of the elliptical roller damper was meticulously recorded by sensors, registering a value of 160 kN, as shown in Fig. 10. The specimens have not failed and no loss of stiffness and strength was recorded. Additionally, the vertical load applied during the test was continuously displayed and monitored through sensors on the display, ensuring accurate tracking of the force exerted. The loading plates are 20 millimeters thick and two sets of three rollers were placed between the vertical loading plate and the horizontal loading plate. Wire encoder along the horizontal actuator is set with an accuracy

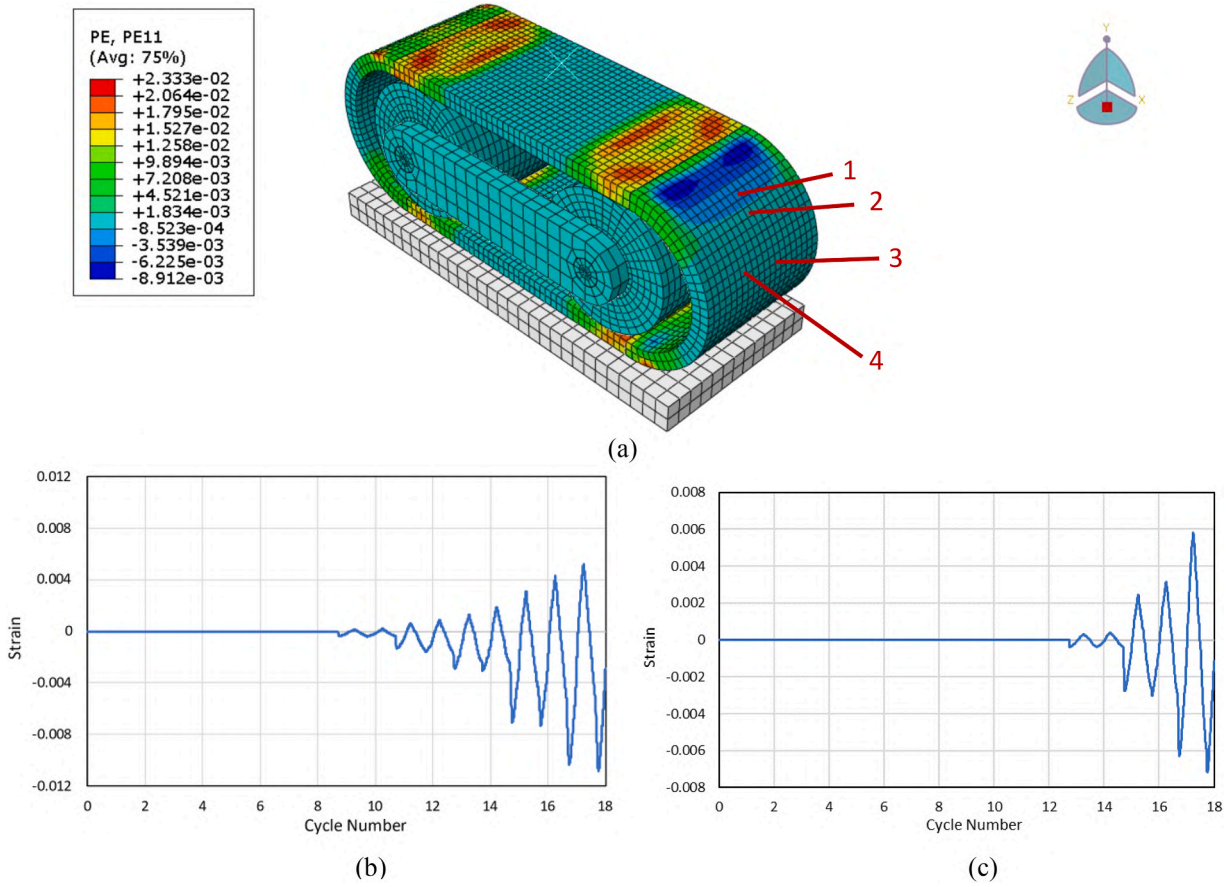

Fig. 17. Plastic Strain: (a) Contour of PE11 at the end of analysis, (b) Strain of elemnt 1 per cycle, (c) Strain of element 2 per cycle.

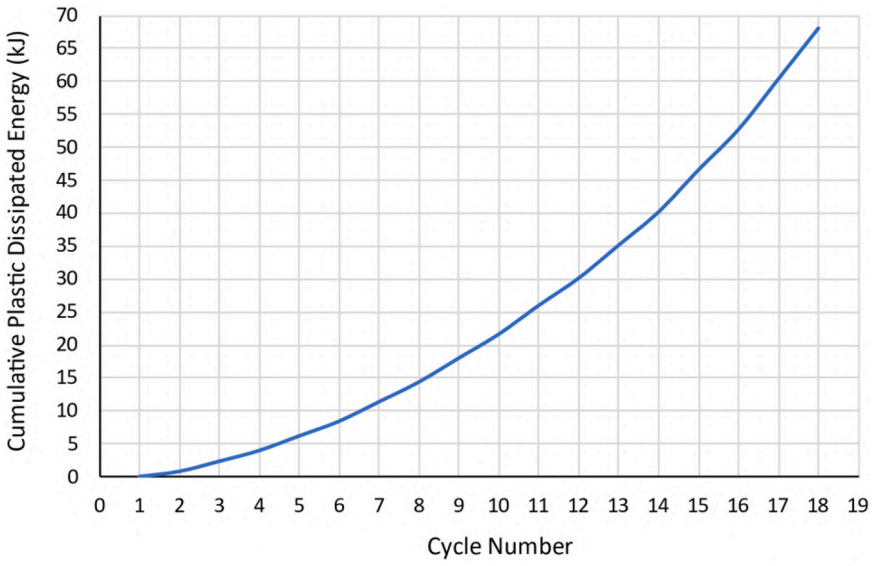

Fig. 18. Cumulative Plastic Dissipated Energy Curve.

of 0.1 mm. The hysteresis curves for each damper, illustrating half the total lateral strength, are depicted in Fig. 11 (a) and (b). The curves generated from these tests display a stable and robust pattern, clearly demonstrating the dampers' capability to dissipate significant amounts of energy. In the second experiment, four strain gauges were attached to one of the dampers, and an LVDT was added for more precise measurement of displacements. The results from the strain gauges are shown in Fig. 11 (c) to (f). It should be noted that strain gauges 1–3 are positioned in the direction of the damper's movement, while strain gauge 4 is positioned perpendicular to the damper's movement.

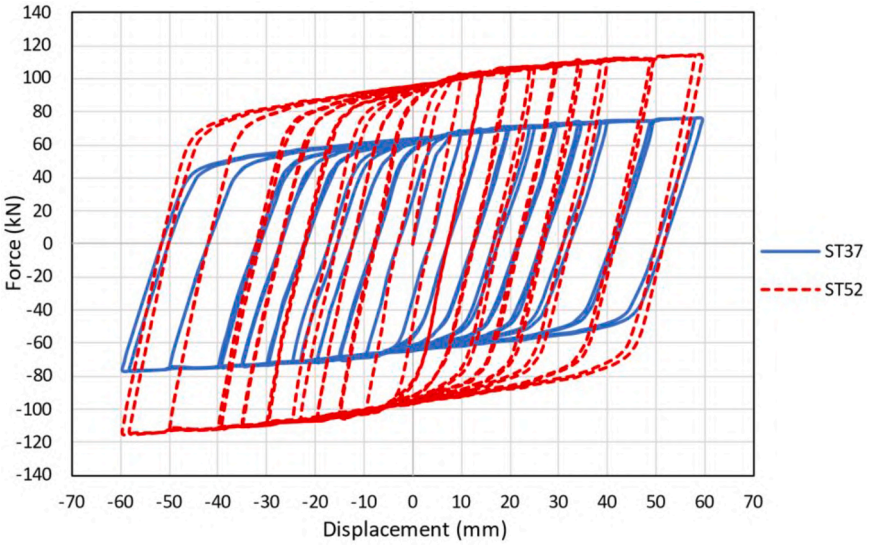

Fig. 19. Comparison of Hysteresis Curve of the Damper with ST37 and ST52.

4. Numerical model

The geometry of the damper was constructed and meshed in the Abaqus software [33,34] according to the dimensions shown in Fig. 6. The mesh size sensitivity analysis was performed based on the mesh size of the elliptical section and the lateral strength of the damper, as shown in Fig. 12. The mesh sizes selected were 5 mm for the elliptical section, rollers, and pins, and 10 mm for the connecting plate and loading plate.

To achieve a more accurate representation of ST37 steel behavior in finite element analyses, the true stress-strain curve for this material has been calculated and included in Fig. 13 (a). This curve was derived from engineering stress-strain data obtained from the tensile test by applying standard transformations to compute true stress and true strain. In these transformations, true stress is calculated using Eq.1, while true strain is calculated using Eq.2. The hardening behavior was selected as kinematic based on the experimental results. In kinematic hardening model, as shown in Fig. 13 (b), the size of the yield surface remains constant, but its center shifts. Additionally, the loading plates were defined as rigid. The model constructed in Abaqus is shown in Fig. 14.

$$\sigma_{true} = \sigma_{engineering}\left(1 + \epsilon_{engineering}\right) \tag{1}$$

$$\epsilon_{true} = \ln\left(1 + \epsilon_{engineering}\right) \tag{2}$$

In the numerical model, all welded components were tied together to reflect their fixed connections in the actual experiment. Similarly, the rod within the cylinder, which was riveted to the connecting plate between the rods in the experiment, was also tied in the model. Surface-to-surface contact was set up between the remaining pairs of plates, with a friction coefficient of 0.2 assumed for interactions between steel members, and these members were further constrained in the out-of-plane direction. Additionally, the end of the bottom plate was fixed in all six directions.

For the simulation of loading conditions, an 180-kN gravity load was first applied as a concentrated compressive force on the top loading plate. Subsequently, a lateral force was applied in a displacement-controlled manner across 18 cycles to the top plate. The resulting hysteresis curve from this analysis, along with a comparison to the experimental hysteresis, is depicted in Fig. 15.

The numerical model developed in this study successfully predicts the initial stiffness and ultimate strength of the specimens. However, it demonstrates a noticeable limitation in accurately capturing the location of stiffness reduction. Despite extensive efforts to address this issue—such as refining mesh sizes, modifying material properties, and recalibrating boundary conditions—the predicted results remained consistent.

This limitation appears to be related to the intrinsic capabilities of the computational framework used (Abaqus). Similar discrepancies have been reported in previous studies employing Abaqus for modeling the behavior of steel structures under similar loading conditions. For instance, studies by [7], [14], and [17] have identified comparable challenges in predicting the stiffness reduction behavior.

While this limitation does not compromise the model's ability to predict global behavior (e.g., initial stiffness and ultimate strength), it highlights the need for further advancements in computational methods to improve the local accuracy of stiffness reduction predictions. This issue is explicitly acknowledged to ensure transparency and to guide future research in this area.

Other results obtained from the numerical analysis are shown in Figs. 16 through 18. Fig. 16 shows the deformed shape of the damper obtained from the finite element model at the maximum displacement of 60 mm. Since no failure was observed during the experimental tests, failure was not modeled in the numerical simulation either.

Numerical strains are presented in Fig. 17, demonstrating good range agreement between the numerical and experimental results. Element 1–4 in numerical model represent strain gauge no. 1–4. However, Abaqus could not predict behavior of gauage no. 3 and 4 and the strain values remain at zero.

Based on the high PEEQ values observed at the specific points highlighted in Fig. 16 (b), it can be concluded that the damper is capable of withstanding significant strain levels without failure. However, it is predicted that these areas would experience failure if cyclic loading countinues.

5. Parametric analysis

The next step in the study is to conduct a parametric analysis, which involves altering key variables by ± 10 %, ± 20 %, ± 30 %, ± 40 %, and ± 50 % from their baseline values in the numerical model. This process allows for the assessment of how changes in these variables influence the damper's performance. Following this analysis, the variables that most significantly affect the energy absorption capabilities of the elliptical roller damper will be ranked. These include the materials used, the magnitude of gravitational load, the length and width of flat plates, their thickness, the curvature radius of the curved section, and the friction coefficient.

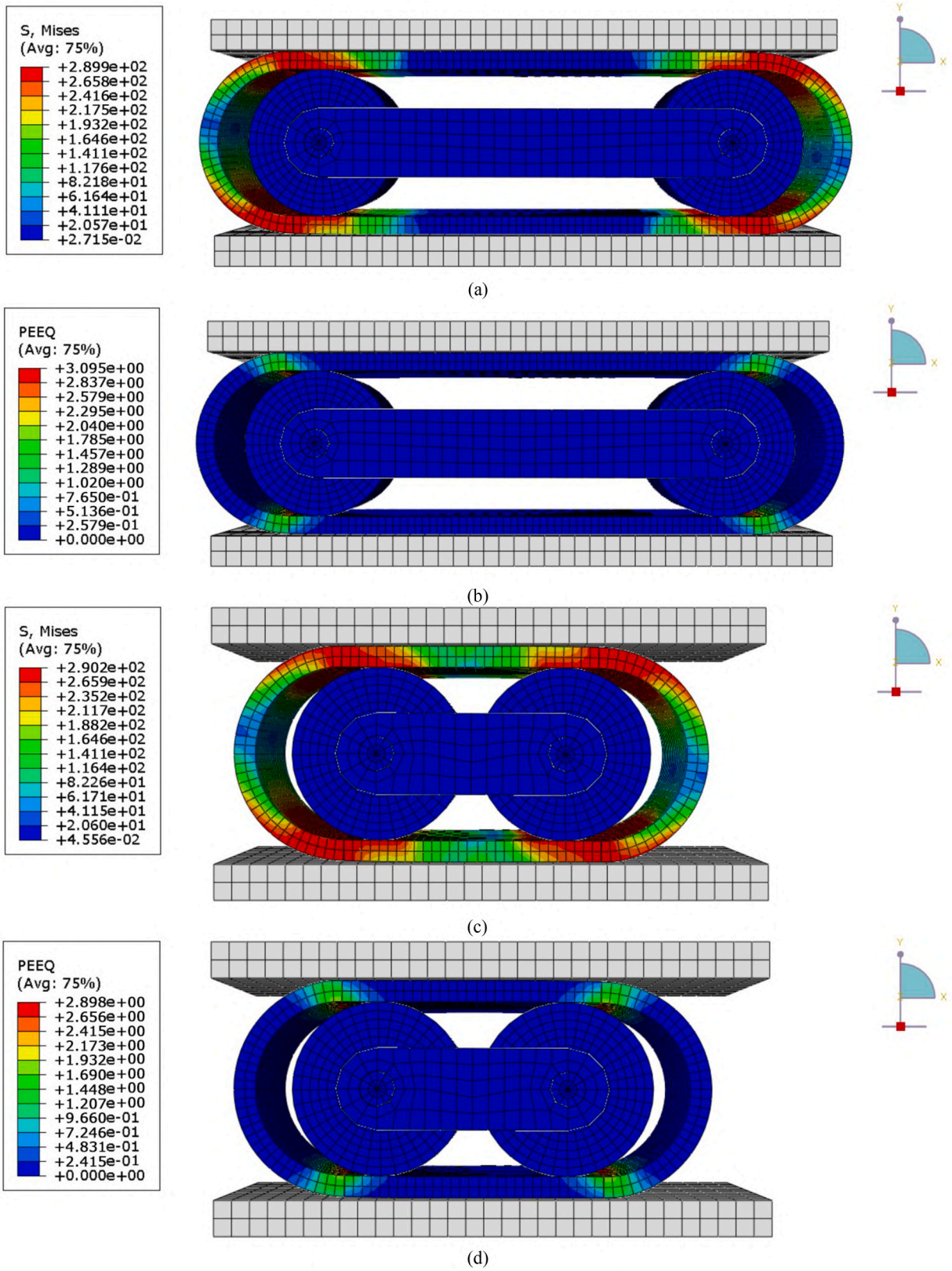

Fig. 20. Equivalent von Mises stress and plastic strain at the end of analysis due to length change:(a) Stress at 150 % of initial length, (b) Strain at 150 % of initial length, (c) Stress at 70 % of initial length, (d) Strain at 70 % of initial length.

5.1. Effect of materials

The impact of material changes on the damper's behavior was specifically evaluated by switching the material in the finite element model to steel ST52, which has a yield stress of 355 MPa and an ultimate tensile strength of 520 MPa. This alteration enhanced the lateral strength of the damper by 50 %, as evidenced in the modified hysteresis curve shown in Fig. 19.

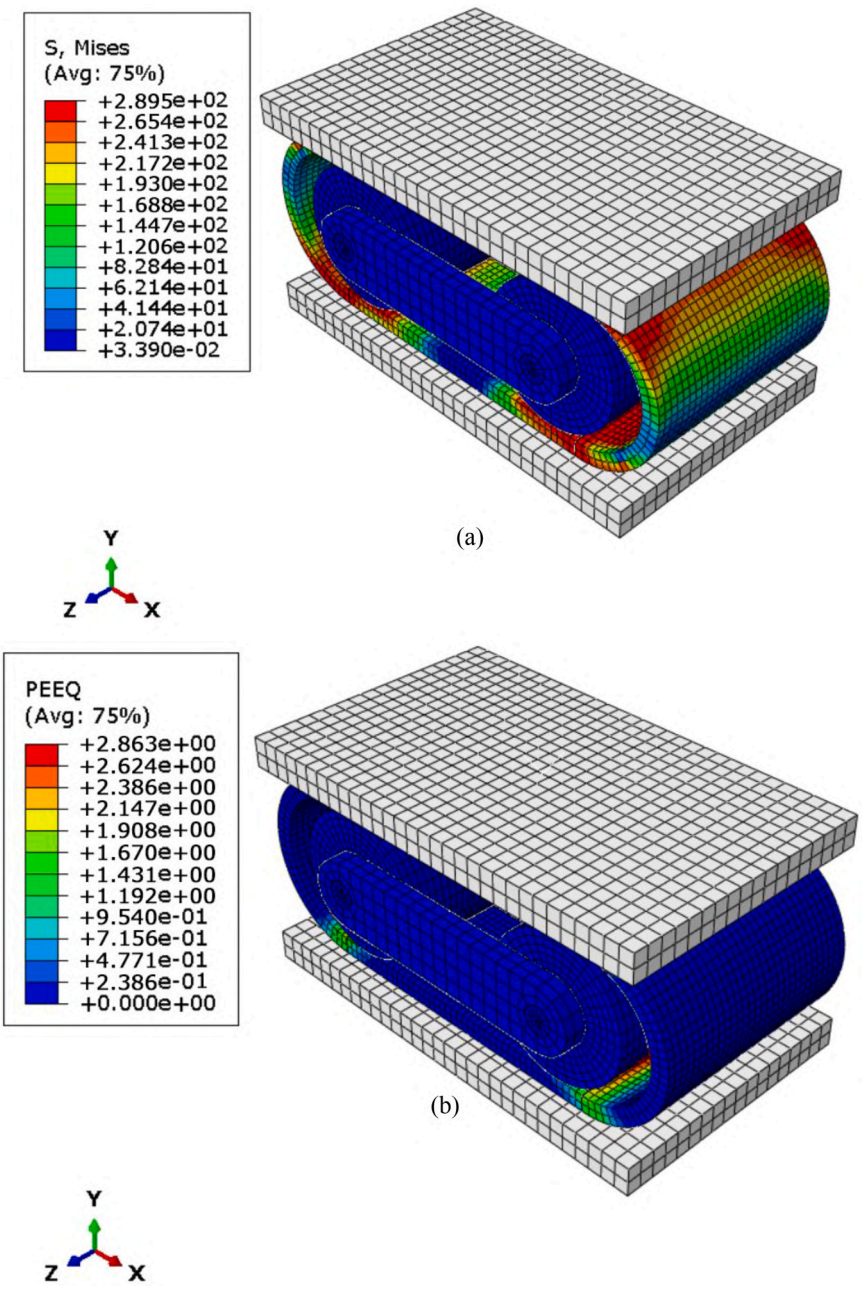

Fig. 21. Equivalent von Mises stress and plastic strain at the end of analysis due to width change: (a) Stress at 150 % of initial width, (b) Strain at 150 % of initial width, (c) Stress at 50 % of initial width, (d) Strain at 50 % of initial width.

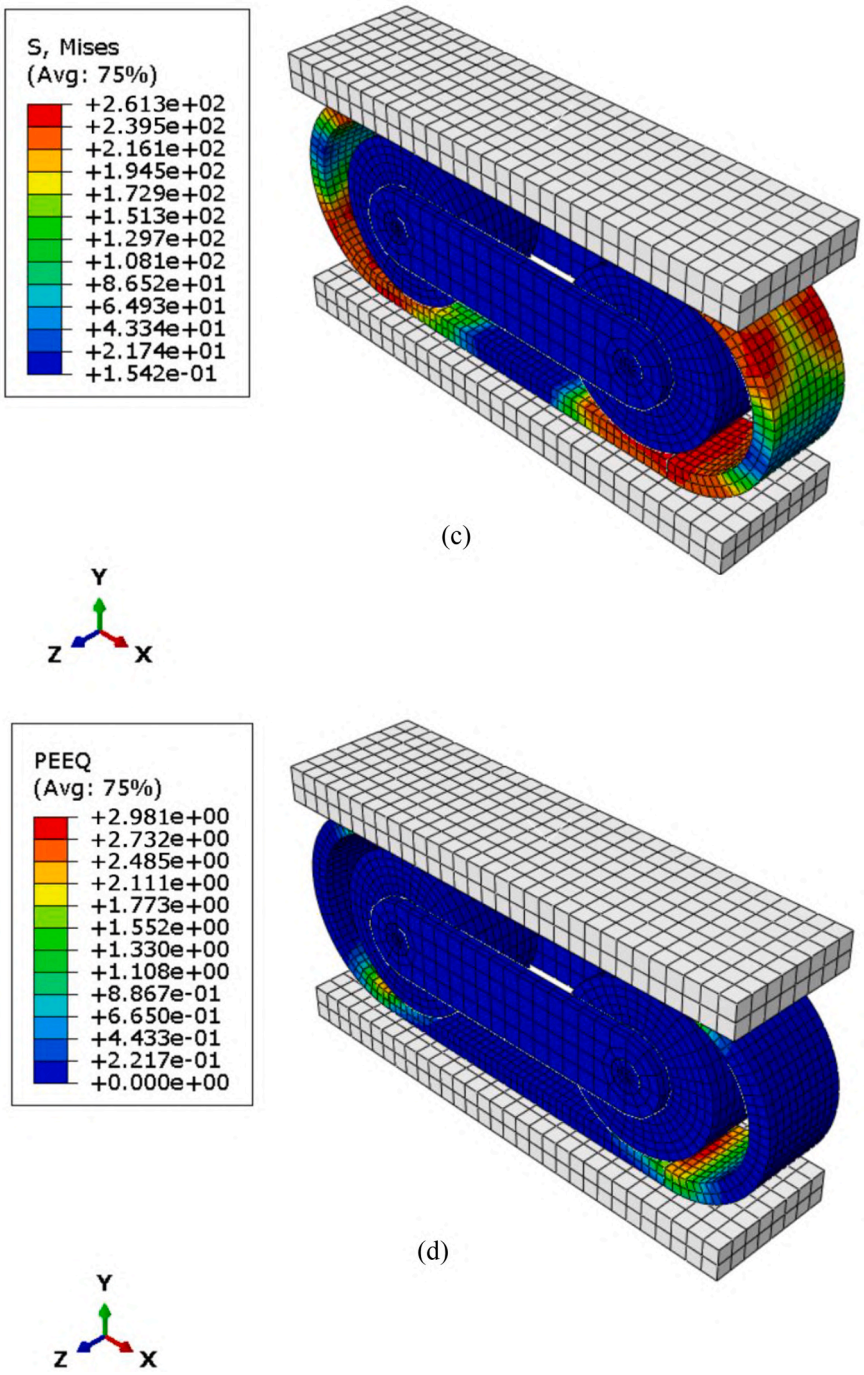

Fig. 21. (*continued*).

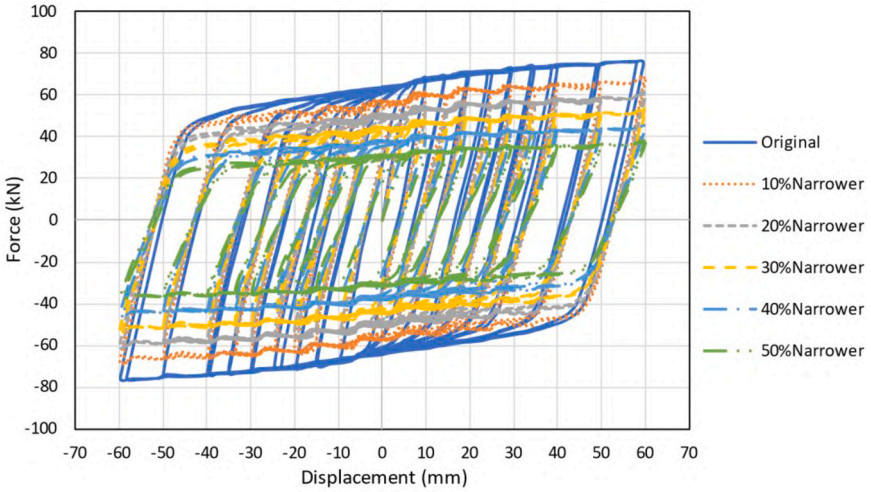

Fig. 22. The effect of decreasing the damper width on the hysteresis curve.

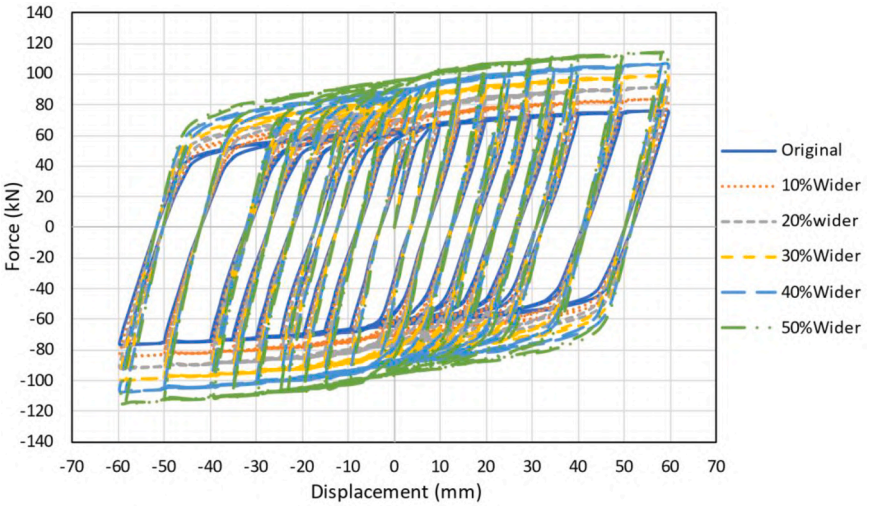

Fig. 23. The effect of increasing the damper width on the hysteresis curve.

5.2. Effect of friction coefficient

The friction coefficient within the models was increased to 0.3, 0.4, and 0.5 in separate simulations to assess its influence on the hysteresis behavior of the damper. However, these changes did not produce a significant impact on the hysteresis curve. This outcome indicates that the rolling action of the rollers interacting with the elliptical section effectively counteracts the effects of increased friction. Thus, within the tested range, the friction coefficient does not substantially alter the damper's performance, showcasing the design's robustness against variations in friction levels.

5.3. Effect of gravity load

The relationship between the gravity load and the lateral strength of the damper was directly tested. The experimental setup varied the gravitational force from 50 % of the original load (90 kN) to 150 % of the original load (270 kN). Results indicated that these variations did not alter the hysteresis curve. The unchanged hysteresis curve despite variations in gravity load and friction coefficient demonstrates that the gravitational load-bearing system operates independently of the lateral load-bearing system.

5.4. Effect of length of flat plates

The numerical study also explored how changes in the length of the flat plates affect the lateral strength of the damper. The length was adjusted incrementally from 70 % of its original length (146 mm) to 150 % (313 mm), increasing by 10 % in each model iteration, as illustrated in Fig. 20. These modifications showed no impact on the hysteresis curve. The decision not to reduce the length to 50 % and 60 % of its initial value was based on the lack of sufficient space to accommodate two rollers. The finding that altering the length of the flat plates does not affect the damper's hysteresis curve is linked to the flat plates' non-yielding characteristics and their minimal role in energy dissipation.

5.5. Effect of width

The impact of varying the width of the damper was numerically tested by adjusting the width both downwards and upwards from its initial measurement, as outlined in Fig. 21. When the width was decreased by 10 %, 20 %, 30 %, 40 %, and 50 % from the original dimensions, the lateral strength of the damper correspondingly diminished by 10 %, 20 %, 30 %, 40 %, and 50 %, respectively, as detailed in Fig. 22. Conversely, increasing the width by the same increments led to an equivalent increase in lateral strength, ranging from 10 % to 50 %, as

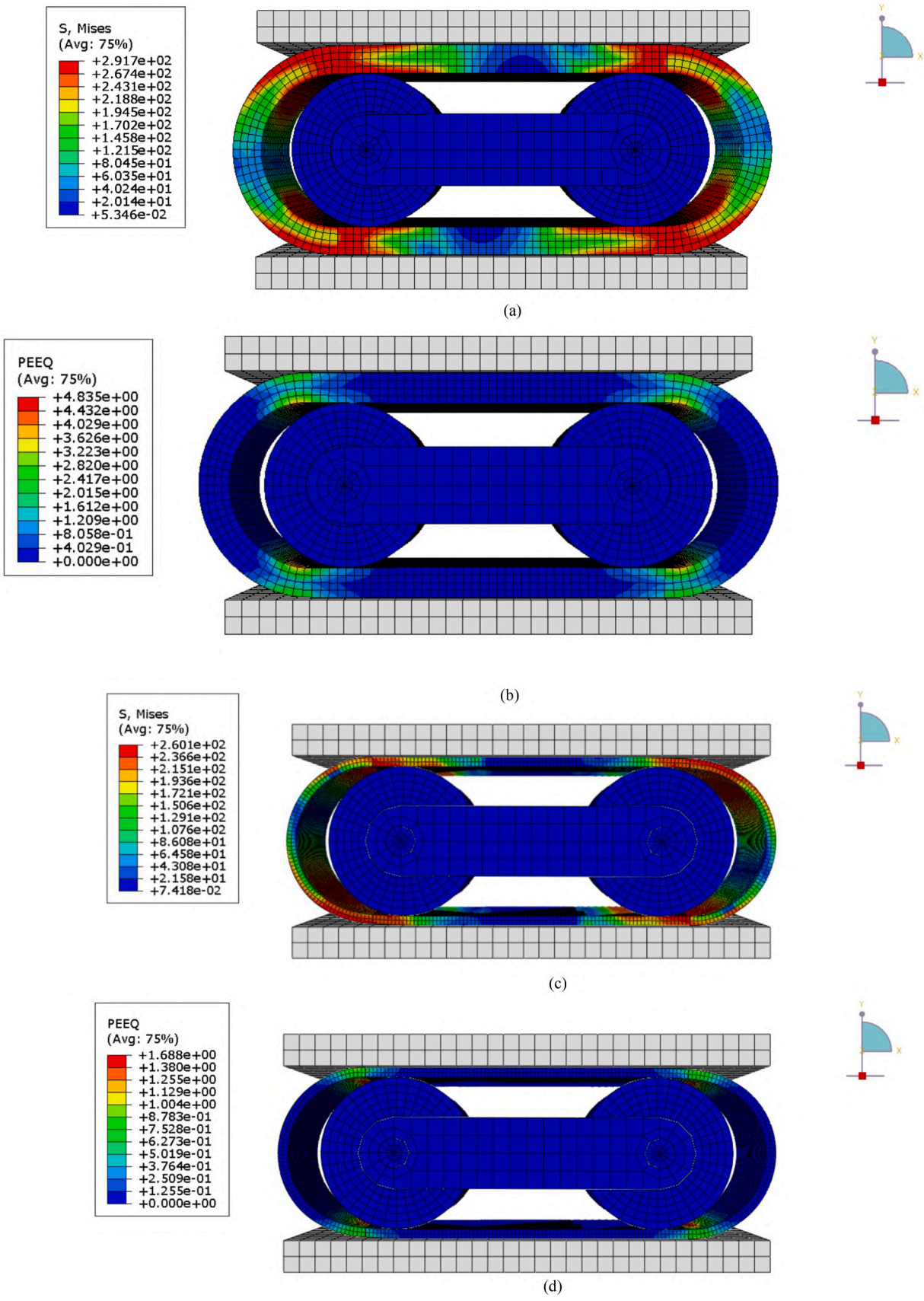

Fig. 24. Equivalent von Mises stress and plastic strain at the end of analysis due to thickness change: (a) Stress at 150 % of initial thickness, (b) Strain at 150 % of initial thickness, (c) Stress at 50 % of initial thickness, (d) Strain at 50 % of initial thickness.

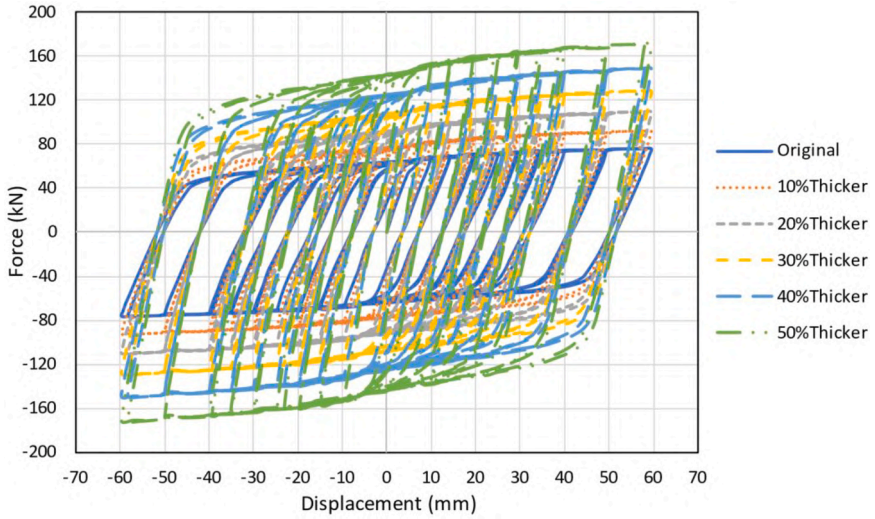

Fig. 25. The effect of increasing the elliptical thickness on the hysteresis curve.

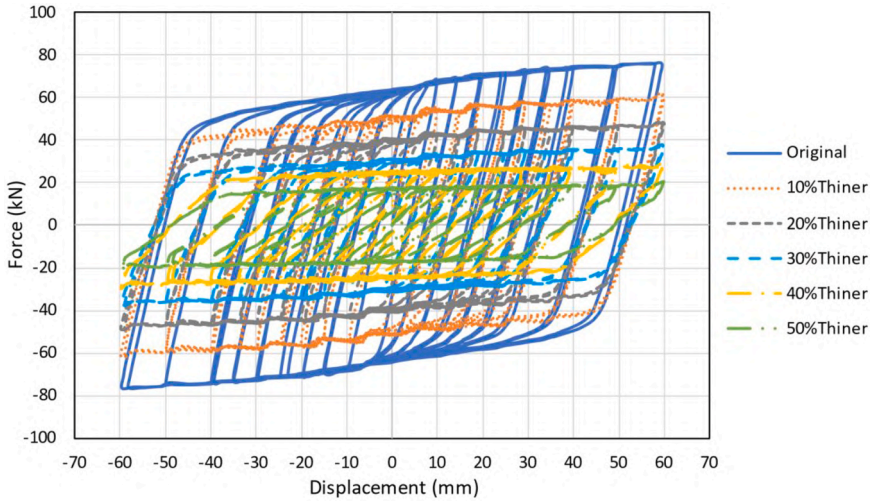

Fig. 26. The effect of decreasing the elliptical thickness on the hysteresis curve.

depicted in Fig. 23. The variations in lateral strength associated with changes in the damper's width are attributed to alterations in the plastic section of the damper that is explained in Eq.3.

$$Z = \frac{bt^2}{4} \tag{3}$$

5.6. Effect of elliptical part thickness

The impact of changing the thickness of the elliptical part of the damper was rigorously evaluated. Variations ranged from 50 % of the initial value (6 mm) to 150 % (18 mm), as depicted in Fig. 24. These modifications resulted in exponential changes in the damper's lateral strength. Specifically, a 50 % increase in thickness led to 225 % of initial lateral strength, while a 50 % reduction in thickness caused 25 % of initial lateral strength, as shown in Figs. 25 and 26.

At the lower thickness settings of 6 mm and 7.2 mm, corresponding to 40 % and 50 % of the initial value, respectively, the simulation failed to produce suitable hysteresis behavior. To address this, the mesh size for the elliptical part of the damper was adjusted to 2.5 mm, as illustrated in Fig. 24. This adjustment resulted in higher stiffness and a steeper decay slope in strength for these configurations compared to others. The observed changes in lateral strength with the varying thickness are due to alterations in the plastic section modulus in Eq.1. The effect of thickness variations on the damper's performance is notably more significant than changes in width, highlighting the critical importance of thickness in the design and functionality of the damper.

5.7. Effect of curve radius (Height)

The curvature radius, which affects the height of the damper, was adjusted from 50 % to 150 % of its initial value, as shown in Fig. 27. This alteration had a significant impact on the lateral strength of the damper: as the radius (height) increased, the lateral strength correspondingly decreased, and it increased as the radius decreased. Changes in height and changes in lateral resistance were inversely related. Specifically, as shown in Figs. 28 and 29, reducing the height led to disproportionately larger increases in strength. When the height was varied to 150 %, 140 %, 130 %, 120 %, 110 %, 90 %, 80 %, 70 %, 60 %, and 50 % of the initial value, the changes in lateral strength observed were approximately 67 %, 73 %, 78 %, 84 %, 92 %, 112 %, 126 %, 143 %, 166 %, and 200 % of the initial value, respectively.

The inverse relationship between the lateral strength and the curve radius is illustrated in Fig. 30 and that is $F_p = \frac{2M_p}{D_u}$.

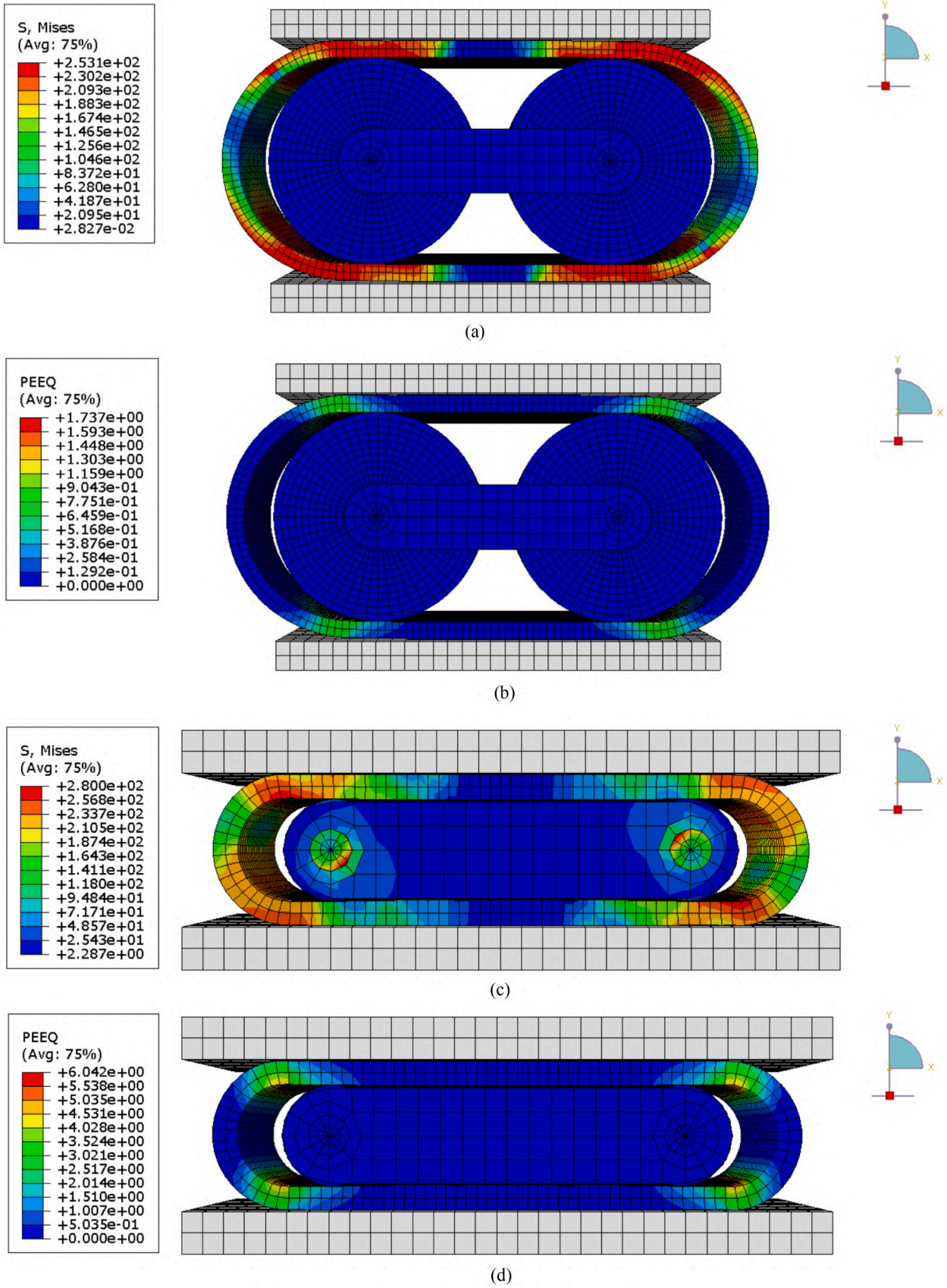

Fig. 27. Equivalent von Mises stress and plastic strain at the end of analysis due to radius change: (a) Stress at 150 % of initial radius, (b) Strain at 150 % of initial radius, (c) Stress at 50 % of initial radius, (d) Strain at 50 % of initial radius.

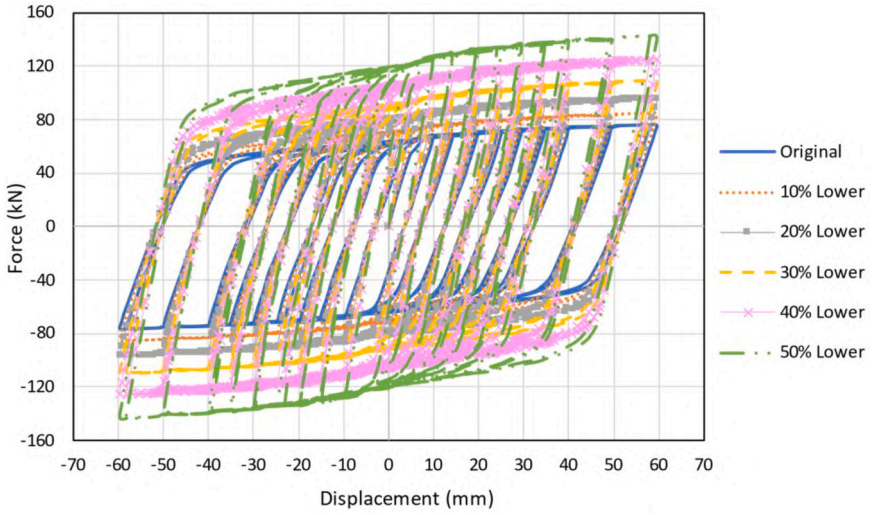

Fig. 28. The effect of decreasing radius on the hysteresis curve.

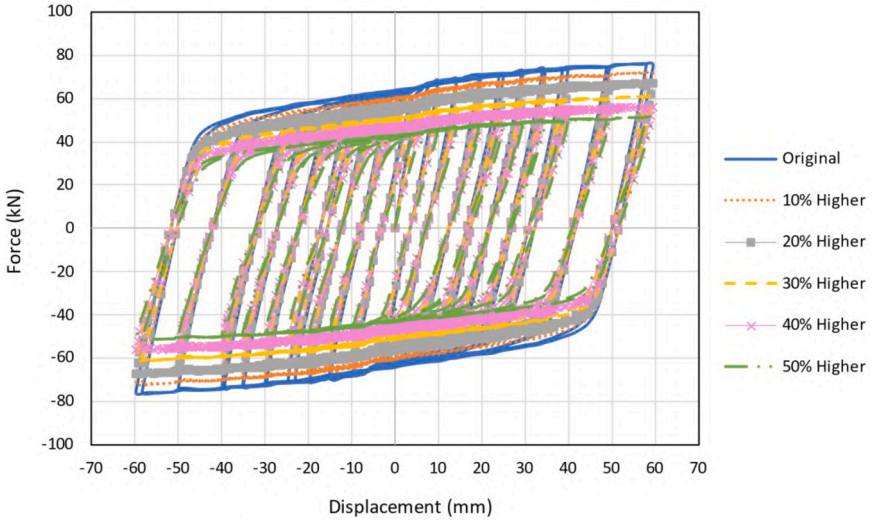

Fig. 29. The effect of increasing radius on the hysteresis curve.

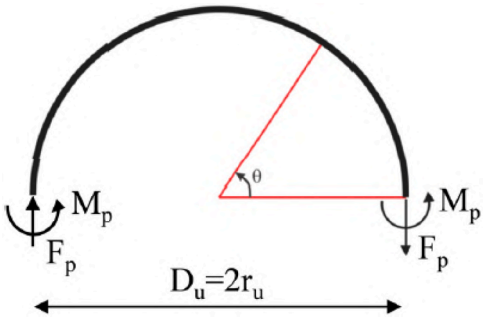

Fig. 30. The relationship between lateral strength and the radius of curvature [6].

6. Conclusion

In this study, an innovative damper was introduced by incorporating rollers into the conventional elliptical design. This elliptical roller damper is designed to effectively dissipate energy from seismic activities while also supporting gravitational loads, thus serving dual functions in both gravity and lateral load-bearing systems. Experimental evaluations confirmed that the damper maintains stable hysteresis behavior and demonstrates commendable energy dissipation capabilities. Further, a numerical model of the damper was developed using Abaqus software. The results from this model closely aligned with those observed in the experimental studies, validating the accuracy of the numerical approach.

The effects of varying several parameters on the damper's hysteresis curve were investigated by adjusting the material, gravitational load, friction coefficient, and dimensions of the damper to 50–150 % of their initial values:

1. The substitution of the material to ST52, which possesses a higher yield stress, resulted in a substantial increase in lateral strength, underscoring the importance of material selection in enhancing the damper's response to seismic loads.
2. Variations in gravitational load and friction coefficient showed minimal influence on the hysteresis curve, suggesting consistent behavior across structures of varying weights and floor levels.
3. Alterations in the length of the flat sections had little effect on the damper's behavior, indicating a lesser role of this dimension in energy dissipation.

4. Modifications in width and thickness revealed that decreasing these dimensions reduces lateral strength, whereas increasing them significantly enhances force tolerance. Notably, changes in thickness had a more significant impact than width adjustments, with the change in strength being exponential to the change in thickness and proportional to width changes.
5. Height adjustments demonstrated an inverse relationship with lateral strength, where reducing height notably improved performance.
6. Examination of stress and strain contours across varied geometries showed minimal differences in stress levels, indicating that geometric changes do not substantially alter stress within the damper. However, variations in height and thickness influenced strain, and drastic reductions in thickness affected initial stiffness.
7. The results obtained from the effect of changes in the geometry of roller dampers on their lateral strength are consistent with those of conventional elliptical dampers. Additionally, changes in gravitational load and friction coefficient do not affect the damper's strength. From these observations, it can be concluded that the gravitational load-bearing system and the lateral load-bearing system in this damper operate independently and do not influence each other.

These findings highlight the critical role of precise dimensional design in optimizing damper performance under actual conditions, providing valuable insights for future enhancements of damper designs.

CRediT authorship contribution statement

Majid Latifi: Resources, Funding acquisition, Data curation, Conceptualization. **Nader Fanaie:** Visualization, Validation, Supervision, Methodology. **Hadis Vakili Sadeghi:** Writing – review & editing, Writing – original draft, Software, Resources, Project administration, Formal analysis.

Declaration of Competing Interest

The authors whose names are listed immediately below certify that they have no affiliations with or involvement in any organization or entity with any financial interest (such as employment, patent-licensing arrangements, etc.), or non-financial interest (such as personal or professional relationships, affiliations, knowledge or beliefs) in the subject matter discussed in this manuscript

Acknowledgments

The authors wish to express their sincere gratitude to the Foolad Machine Neka company for their invaluable support throughout the experimental phases of this study. The facilities and resources provided by Foolad Machine Neka company were instrumental in conducting the comprehensive tests necessary to evaluate the performance of the elliptical roller damper. Special thanks are also extended to the technical staff and engineers whose expertise and dedication greatly contributed to the success of this research.

References

[1] "Minimum Design Loads and Associated Criteria for Buildings and Other Structures (ASCE/SEI 7–22)."
[2] "NEHRP Recommended Provisions: Instructional Materials (FEMA 451B)."
[3] Kelly JM, Skinner RI, Heine AJ. Mechanisms of Energy Absorption in Special Devices for Use in Earthquake Resistant Structures. Bull N Zeal Soc Earthq Eng 1972;5(3):63–73. https://doi.org/10.5459/bnzsee.5.3.63-88.
[4] Skinner RI, Kelly JM, Heine AJ. Hysteretic Dampers for Earthquake-Resistant Structures. Earthq Eng Struct Dyn 1974;3(3):287–96. https://doi.org/10.1002/eqe.4290030307.
[5] Qu B, Daia C, Qiua J, Houa H, Qiu C. Testing of seismic dampers with replaceable U-shaped steel plates. no. August 2018 Eng Struct 2018;179:625–39. https://doi.org/10.1016/j.engstruct.2018.11.016.
[6] A. Baird, T. Smith, A. Palermo, and S. Pampanin, "Experimental and Numerical Study of U-shape Flexural Plate (UFP) Dissipators," in NZSEE, 2014.
[7] Deng K, Pan P, Su Y, Xue Y. Shape optimization of U-shaped damper for improving its bi-directional performance under cyclic loading. Eng Struct 2015;93:27–35. https://doi.org/10.1016/j.engstruct.2015.03.006.
[8] Kim S, Kim K-H. Evaluation of structural behavior of hysteretic steel dampers under cyclic loading. Appl. Sci 2020.
[9] Taiyari F, Mazzolani FM, Bagheri S. A proposal for energy dissipative braces with u-shaped steel strips. J Constr Steel Res 2019;154:110–22. https://doi.org/10.1016/j.jcsr.2018.11.031.
[10] Mazzolani FM, Taiyari F. The influence of the U-shaped damper configuration on the seismic performance of steel building frames. 10th Int Conf Behav Steel Struct Seism Areas 2022:650–8.
[11] C. Lee, Y. Wang, and M. Cai, "An Experimental Study of In - plane Oval Damper," in 3rd World Congress on Civil, Structural, and Environmental Engineering (CSEE'18), 2018, doi: 10.11159/icsenm18.110.
[12] Gao J, Xi J, Xu Y, Ding J, Zhu J, Chang Y, et al. Analysis of the mechanical properties and parameter sensitivity of a U-shaped steel damper. Front Mater 2021;8.
[13] Satria E, Son L, Bur M, Akbar MD. Finite element analysis to determine stiffness, strength, and energy dissipation of u-shaped steel damper under quasi-static loading. Int J Automot Mech Eng 2021;18(3):9042–50. https://doi.org/10.15282/ijame.18.3.2021.16.0693.
[14] Ebadi Jamkhaneh M, Ebrahimi AH, Shokri Amiri M. Experimental and numerical investigation of steel moment resisting frame with u-shaped metallic yielding damper. Int J Steel Struct 2019;19(3):806–18. https://doi.org/10.1007/s13296-018-0166-z.
[15] Bakhshpoori T, Masoumnejad M. Performance evaluation of U-shaped metallic-yielding damper in RC frames irregular in elevation. MCEJ 2022;22(2):75–87.
[16] Bagheri S, Barghian M, Saieri F, Farzinfar A. U-shaped metallic-yielding damper in building structures: seismic behavior and comparison with a friction damper. Structures 2015. https://doi.org/10.1016/j.istruc.2015.04.003.
[17] Chen Y, Chen C, Jiang H, Liu T, Wan Z. Study of an innovative graded yield metal damper. J Constr Steel Res 2019;160:240–54. https://doi.org/10.1016/j.jcsr.2019.05.028.
[18] Varzaneh MNajari, Hosseini M, Akbarpoor A. The study of EADAS elliptical steel damper function in seismic resisting of steel frames. J Rehabil Civ Eng 2014;2:40–5.
[19] Najaf E., Abbasi H., Orouji M. 2021. Evaluation of the Performance of Ring-Shaped, Elliptical, and T-Adas Yielding Dampers in Chevron Braci.
[20] Bursi OS, Fanaie N, Safaei Faegh S, Sepasgozar Sarkhosh O. An improved cable-cylinder bracing system with quarter-ring yielding devices for seismic retrofit of steel moment frames. Bull Earthq Eng 2021;19(9). https://doi.org/10.1007/s10518-021-01108-x.
[21] Maleki S, Mahjoubi S. Dual-pipe damper. J Constr Steel Res 2013;85:81–91. https://doi.org/10.1016/j.jcsr.2013.03.004.
[22] Maleki S, Mahjoubi S. Infilled-pipe damper. J Constr Steel Res 2014;98:45–58. https://doi.org/10.1016/j.jcsr.2014.02.015.
[23] Maleki S, Bagheri S. Pipe damper, part I: experimental and analytical study. J Constr Steel Res 2010;66(8–9):1088–95. https://doi.org/10.1016/j.jcsr.2010.03.010.
[24] Maleki S, Bagheri S. Pipe damper, part II: application to bridges. J Constr Steel Res 2010;66(8–9):1096–106. https://doi.org/10.1016/j.jcsr.2010.03.011.
[25] Suzuki K, Watanabe A, Saeki E. Development of U-shaped steel damper for seismic isolation system. Nippon Steel Tech Rep 2005;(92):56–61.
[26] Oh S, Song S, Lee S, Kim H. Seismic response of base isolating systems with U-shaped hysteretic dampers. Int J Impact Eng 2012;12(2):285–98. https://doi.org/10.1007/s13296-012-2011-0.
[27] S. Vamshisheela and A. Manchalwar, "Isolating System using U Shaped Steel Damper," in 3rd International Conference on Design and Manufacturing Aspects for Sustainable Energy, 2021.
[28] R.S. Henry, S. Aaleti, S. Sritharan, and J.M. Ingham, "Design of a Shear Connector for a New Self-Centering Wall System," in The 14th World Conference of Earthquake Engineering. Beijing, 2008.
[29] Kim H-J, Choi K-S, Oh S-H, Kang C-H. Comparative study on seismic performance of conventional rc coupling beams and hybrid energy dissipative coupling beams used for RC shear walls. 15th World Conf Earthq Eng (15WCEE) 2012.
[30] Aydenlou RM. Seismic Rehabilitation Methods for Existing Buildings (Butterworth-Heinemann). Oxford: Elsevier; 2020. https://doi.org/10.1016/C2018-0-05546-2.
[31] ASTM International. ASTM E8/E8M-13a: Standard test methods for tension testing of metallic materials. West Conshohocken, PA: ASTM International; 2013.
[32] "Interim Testing Protocols for Determining the Seismic Performance Characteristics of Structural and Nonstructural Components (FEMA 461)," no. June. 2007.
[33] SIMULIA, Abaqus User's Manual. Rhode Island, USA: Version 6.14, Dassault Systèmes Simulia Corp, 2014.
[34] Meghdadi Z, Khaloo A. Experimental, theoretical and numerical study on flexural behavior of hybrid steel-GFRP reinforced concrete slabs. Struct Concr 2024. https://doi.org/10.1002/suco.202301085.